Modelling the performances of an innovative shading device integrating PV

Emanuele Piccoli[1], Alessandro Dama[2]
[1]Empa, Dübendorf, Switzerland
[2]Politecnico di Milano, Milan, Italy

Abstract

This study presents a first assessment of the overall energy performances of a novel BIPV façade systems. Specifically, it focuses on an innovative extensible louvre integrating PV. A suitable optical model was developed, and validated against Window software, for characterizing the bidirectional properties of the complex fenestration system (CFS), having a peculiar shading geometry and combination of PV and blind surfaces. The CFS characterization and the control strategy, for regulating louvre tilt and extension, were implemented in EnergyPlus via EMS, for simulating heating cooling and lighting needs. PV generation was modelled taking into account partial shading effects. The integrated building and PV simulation and the introduction of an overall energy performance index allow to optimize the control strategy. The results show that for a South facing typical office module in Milan the new BIPV system, beside the relevant RES exploitation, is able to provide effective solar control, without compromising daylighting.

Introduction

In the perspective of new Zero Energy Buildings, the exploitation of RES is a key issue. In this regard, the integration of photovoltaic components in the building envelope, not only in the roof but also in façade, will play an important role. In this context, new developments in integrated simulation tools are necessary to support the design, use and optimization of building integrated photovoltaics (BIPV) technologies.

Peng et al. (2017) demonstrated that window attachments have a large impact on building energy performance and that the use of indicators to relatively quantify the benefits of solar shadings in both heating and cooling seasons is of crucial importance for a correct energy rating. Following this path, this work analyses the integrated performance of external shading systems integrating photovoltaics (PV).

In fact, this paper focuses on the development of an optical and PV model, integrable with a building simulation tool, to evaluate and optimize the integrated performances of an innovative BIPV system, which consists in external orientable and extensible PV louvers (Piccoli and Dama 2018).

The novel louvers extension mechanism allows the system to provide effective solar control while increasing the exploitation of daylighting and solar gains with respect to a traditional louvre system: indeed, with the extension of the lamellas the beam radiation is blocked at will, while the permeability to the sunlight is higher than a traditional system when the lamellas are open.

Due to the peculiar geometrical features of the louvres, an optical model characterizing its properties in form of bidirectional scattering distribution functions (BSDF) was developed, since the available free-to-use and commercial software with this aim, such as Window by LBNL, do not include the possibility to analyse such complex surfaces - i.e. with not uniform reflectance and curvature -, but have the advantage to be integrable with widely diffused building simulation software. For this reason, the developed model produces the same type of output of Window.

In order to accurately predict the energy yield of the PV generators, a dedicated BIPV model including partial shading effects as well as thermal and optical aspects was employed. Such a model describes the effects of mismatching considering the PV cells reverse characteristic and power losses and was experimentally validated in Piccoli et al. (2019).

In order to evaluate the performances and multifunctionality of the new PV shading system, it was applied, as a case study, to a typical office module with a South facing window and simulated in EnergyPlus. The implemented control strategy was based on the external climatic conditions of temperature and solar irradiance.

Finally, daylighting potential, heating and cooling needs reduction and PV production have been evaluated and an overall energy performance indicator has been introduced. It allows to optimize the control strategy thresholds and to evaluate the benefit of the innovative shading device integrating PV.

Resuming, the main novel contributions of the paper concern:

- the development and validation of an extended optical model for complex shading devices;
- the integration in Energy Plus of the novel BIPV system;
- a first assessment of its integrated energy performances.

The building simulation case study and the main features of the optical and of the PV model are presented in Section “Methods”.

Section “Results and discussion” presents the validation of the optical model and the evaluation of the energy performance indicators for the simulated BIPV system.

Methods

The methodology adopted involves the following steps, which are described in this Section.

- The development of an optical model, for the peculiar PV louvre system combined with suitable glazing, for the bidirectional characterization of the complex fenestration system (CFS). Such an optical model will be validated against Window LBNL software for a case with a traditional blind geometry, with uniform curvature and reflectance.
- The integration of the photovoltaic model with the fenestration system one.
- The definition of a building and climate case study, for simulating the building integrated performances and the choice of a reference façade system - based on the requirements of the Regional Standard (from EPBD) - as the benchmark for the energy performances.
- The definition and optimization – for the specific building and climate - of a control strategy for dynamically actuate the tilt angle and the extension of the louvres, based on the following hierarchy priorities: daylighting, solar control and solar energy harvesting.

Optical model

The geometrical features of the moveable PV-louvres systems are presented in Figure 1.

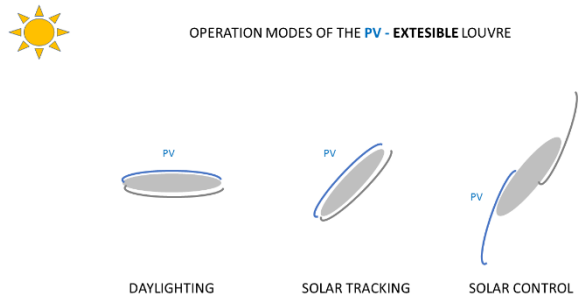

Figure 1 - vertical sections of the extensible louvres in different configuration mode: daylighting, solar tracking and solar control

A PV module is integrated on the upper side of the more external lamella of each extensible louvre. The optical properties of the PV and blind surfaces are reported in Table 2. Both the complex geometry and the mixing of different materials require the development of a model which is able to go beyond the currently available libraries.

Such a model, developed in a Matlab environment, calculates the bidirectional optical properties of the shading and/or of the fenestration system when it is combined with glazing. It is based on the radiosity method, i.e. it assumes purely diffuse reflection on the lamellas.

Table 1 – PV-shading optical properties

PROPERTY	PV	BLIND
Solar reflectance	0.19	0.7
Visual reflectance	0.19	0.7

The procedure used is similar to the one presented by Curcija et al. (2018) and employed by Window software. The same angular matrix base was used in order to produce a comparable output for Window and a suitable input for EnergyPlus (EP). The curved surfaces are approximated as a broken line, the contributions to the transmission (or reflection) through the fenestration “layer” is divided in a direct part, which does not take part to reflections among the lamellas, and a diffuse part, which activates a mutual reflection cascade.

The main difference in the calculation method is the way to solve mutual reflections, where the explicit formulation introduced in Dama and Lastaria (2012) is adopted.

The absorptances of the shading and of the glazing layers in the CFS are calculated from the bidirectional transmittance and reflectance of each individual layer employing - for each pair of layers - the following formulation which accounts for multireflection:

$$\alpha^{*}_{i}{}^{1F} = \alpha_{i}{}^{1F} + \Sigma_{jk}\, \tau_{ij}{}^{1F} \rho_{jk}{}^{2F}\, \alpha_{k}{}^{1B} + \\ + \Sigma_{jklm}\, \tau_{ij}{}^{1F} \rho_{jk}{}^{2F}\, \rho_{kl}{}^{1B}\, \rho_{lm}{}^{2F}\, \alpha_{m}{}^{1B} + \ldots \quad (1)$$

$$\alpha^{*}_{i}{}^{2F} = \Sigma_{j}\, \tau_{ij}{}^{1F}\, \alpha_{j}{}^{2F} + \\ + \Sigma_{jkl}\, \tau_{ij}{}^{1F} \rho_{jk}{}^{2F}\, \rho_{kl}{}^{1F}\, \alpha_{l}{}^{2F} + \ldots \quad (2)$$

Which in matrix formulation respectively give:

$$A^{*1F} = A^{1F} + T^{1F}[1 - R^{2F}\, R^{1B}]^{-1} R^{2F} A^{1B} \quad (3)$$

$$A^{*2F} = T^{1F}[1 - R^{2F}\, R^{1B}]^{-1} A^{2F} \quad (4)$$

Where A^{*} indicates the layer absorptance evaluated in the fenestration system.

PV model

The PV model adopted to estimate the renewable energy production of the BIPV system describes the working characteristic of crystalline silicon modules exposed to partial shading. Such a model takes into account the power losses occurring in the real application due to current or voltage limitation due to a limited sky view and mismatch among the cells (Alonso-Garcìa et al. 2006, Liu et al. 2011), as well as the change in temperature of the cells (i.e. power dissipation across the lamellas).

The simplified version of the model introduced in Piccoli et al. (2019) is particularly suited as implies a low computational effort without jeopardizing the accuracy of the power production results. It consists of a classical five parameter cell model (De Soto et al. 2006) integrating a dynamic 1-D thermal model of the cells and lamella materials. The fastening of the simulations is obtained describing the by-pass diodes as logical on-off switches, while the accuracy is validated with both experimental measurements and detailed electrical modelling. Figure 2 depicts the working principle of the PV model simplification.

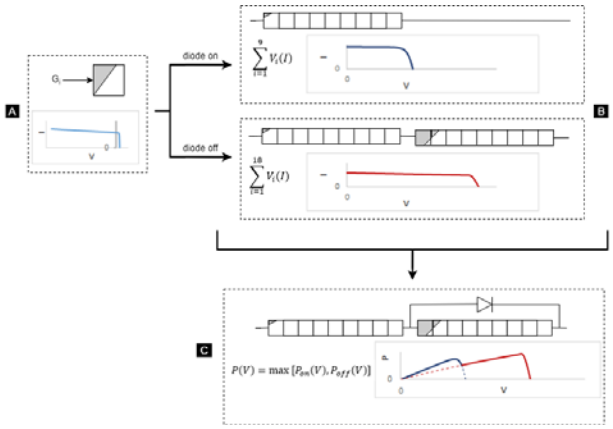

Figure 2 - Graphical representation of the PV model (Piccoli et al. 2019). A) Shadow calculation allows modelling the cell characteristic. B) Two simple arrays are simulated separately requiring low computational effort. C) The array is electrically/ thermally simulated combining the simple characteristics.

Case study

As a case study for evaluating the performances of the new PV shading system a typical office module with a South facing window and the location of Milan were selected.

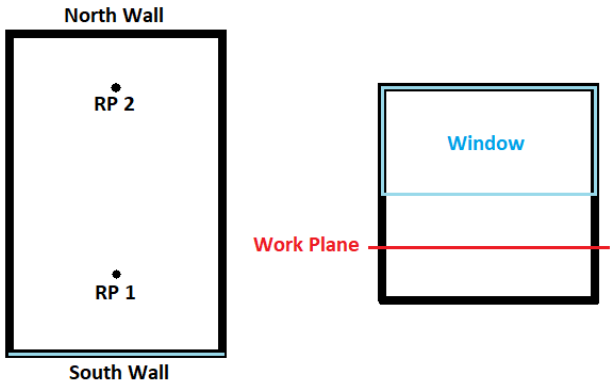

Figure 3 - Top (a) and front (b) view of the building module (positioning of daylighting reference points).

A front and plan view of the office module is drawn in Figure 3. The window to wall ratio is 0.5. The module has only one external wall, all the other walls, floor and ceiling are assumed adiabatic, ventilation is based on occupant schedule and an additional constant infiltration rate is assumed. Simulation of heating and cooling needs are performed using EP v8.5 with Ideal Air System and Economizer. The main specifications for the building simulation are reported in Table 2 and Figure 4.

Table 2 - Main building simulation specifications

Floor area	Wind. area	Heat/Cool setpoints	Heat/Cool attenuation setpoints	Daylighting threshold
13.5 m^2	4.5 m^2	20/26 °C	16/30 °C	600 lux
U_{opaque}	Light. power	Light. control	N.of people & PC	Air infiltr.
0.19 W/m^2K	11 W/m^2	Two steps	2	0.15 Vol./h

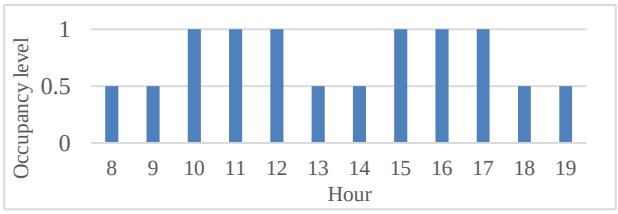

Figure 4 - Relative office occupancy schedule for Weekdays

For the baseline case, a spectrally selective double glazed unit (DGU) was chosen for the fenestration system, without the application of shading. It results in window thermal transmittance below 1.4 $W/(m^2K)$ and solar factor below 0.35, meeting the envelope performance requirements given by the Regional Standard.

The innovative PV louvre system was instead combined with a LowE double glazed unit, with similar thermal transmittance to the baseline, but higher solar and visual transmittance, since the solar control requirement is here satisfied by means of external shading. The properties of the two glazing are reported in Table 3.

Table 3 - Glazing properties – the Spectrally selective DGU employed in the baseline and the Low-E DGU adopted in combination with the external louvre system (optical properties at normal incidence angle)

PROPERTY	SPECTRALLY SELECTIVE	LOW-E
Solar transmittance	0.25	0.42
Visual transmittance	0.58	0.75
Solar factor	0.32	0.50
Thermal transmittance	1.09 $W/(m^2K)$	1.16 $W/(m^2K)$

As for the PV modules implemented in the simulation, it is assumed to implement lightweight, flexible monocrystalline silicon modules, whose equivalent cells main characteristics are gathered in Table 4. The PV cells are disposed over two rows (one forward and one backward), each of them connected in parallel with a by-pass diode in order to improve the performance of the system when the most backward row is shaded.

Considering the building module geometry and the extensible louvre mechanism, the PV area installed is 2.25 m^2, meaning 358 W peak power (26.5 W_{PV}/m^2_{floor}). As the PV is installed only on the window surface, the results can be compared against any semi-transparent BIPV application (e.g. PV glasses, overhangs etc.).

Table 4 - Equivalent PV cells parameters implemented in the simulation

Technology	m-Si
V_{MP}	0.58 V
I_{MP}	8.16 A
P_{MP}	4.73 W

V_{OC}	0.65 V
I_{SC}	8.45 A
Efficiency	15.91%
k_V	-0.33 %/°C
k_I	0.036 %/°C
NOCT	42 °C

The implementation of a dynamic CFS in EP is not straightforward still. Firstly, Delight, the most accurate daylighting engine, is actually not available in the latest versions due to a possible programming bug when dealing with complex shading layers. Therefore, the less accurate SplitFlux method was used instead. Secondly, the Energy Management System (EMS) available calling point happens too late in the program workflow, so that to get an acceptable result with regard to daylighting it is necessary to run simulations with timesteps of five minutes.

Control strategy

The BIPV shading system is actuated through the EMS according to the defined control strategy. Due to the currently available features of EP, it is mandatory to use only CFS-independent input as control parameters. For this reason, instead of illuminance sensors, the device is regulated according to the solar irradiance on the façade and on the external air temperature.

Three possible configuration modes can be actuated (see also Figure 1):

- Daylighting, the lamellas are kept reclosed and horizontal
- Solar tracking, the lamellas are tilted orthogonal to the Sun and reclosed
- Solar control, the lamellas are tilted orthogonal to the Sun and partially or fully extended

Solar tracking is activated anytime the measured vertical irradiance (G_v), is above a threshold (G_{ST}), which is expected to do not conflict with daylighting need.

Whenever free cooling is an available option (i.e. external temperature is below a certain value, which has been fixed 10°C below the cooling setpoint) the solar control priority is neglected in favour of daylighting.

Schematically:

- If the external air temperature is below 16°C
  - If $G_V < G_{ST}$ → daylighting mode
  - If $G_V > G_{ST}$ → solar tracking mode
- If the external air is above 16°C, the lamellas can be extended according to the irradiance level
  - If $G_V < G_{ST}$ → daylighting mode
  - If $G_V > G_{ST}$ → from solar tracking to solar control mode, the extension of the lamellas is proportional to the irradiance exceeding the threshold (maximum extension when vertical irradiance is double the threshold)

The irradiance threshold is dependent on the building type and use (window to wall ratio, internal gains, ventilation strategy…). In this work, the optimal value for the selected case study is found via a parametric analysis of the building performances, as reported in the next Section.

Results and discussion

This section presents and discusses the results of the validation of the developed optical model and the results of the building integrated simulation of the performances of the innovative PV-louvre system.

Both for the model validation and for the performance simulation the external louvres were combined in a CFS with the (lowE) double glazing unit already introduced in the previous section Table 3.

Optical model validation

The optical model used for the generation of the BSDF has been validated comparing the results obtained with the simulation of a CFS composed by a double glazing and a venetian blind with LBNL Window. Four test cases were analysed combining different blind reflectance and different tilt angles. The relevant parameters are resumed in Table 5.

Directional to hemispherical and hemispherical to hemispherical (diffuse) properties are integrated form the bidirectional characterization matrix employing the angular factors ψ_j, as in equation (5) and (6) which define respectively directional to hemispherical and diffuse transmittances:

$$\tau_i = \Sigma_j \, \tau_{ij} \, \psi_j \tag{5}$$

$$\tau_{diff} = (\Sigma_i \, \tau_i \, \psi_i)/\pi \tag{6}$$

where τ_{ij} are the elements of the bidirectional matrix with i and j respectively as incidence and outgoing indexes.

Table 5 - Blind properties in the validation cases

CASE	REFLECTANCE	TILT ANGLE
A	0.7	0°
B	0.7	45°
C	0.3	0°
D	0.3	45°

In order to validate the developed model against Window calculation, two error evaluators have been introduced:

1) max_ΔX, the maximum absolute error of the directional to hemispherical property X_i, among incident directions i,

$$max\_\Delta X = max_i\{|X_i^{model} - X_i^{window}|\} \tag{7}$$

2) WMRE_X, the weighted mean relative error of X

$$WMRE\_X = \frac{\Sigma_i \, |X_i^{model} - X_i^{window}| \psi_i}{\Sigma_i \, X_i^{window} \psi_i} \tag{8}$$

where X can be any window or layer transmittance, reflectance or absorptance.

The results for the main solar properties are gathered in Table 6, while in Figure 5 an example of directional properties distribution is shown. Both representations demonstrate a good agreement of the results with the reference. Cases A and B, in which blind reflectance is higher, present also higher errors. Nevertheless, WMRE

are always within 4% except for the solar front absorbance of the first layer (the Venetian blinds) in Case A, where WMRE is 6%, with max_Δ that achieves 0.1.

Table 6 – maximum absolute and relative errors in modelling the CFS test cases respect to Window

Property	case	A	B	C	D
τ^F	max Δ	0.04	0.05	0.02	0.02
	WMRE	3%	3%	2%	1%
	$\tau_{diff}^{F\ window}$	0.22	0.16	0.18	0.13
ρ^B	max Δ	0.03	0.03	0.01	0.01
	WMRE	2%	4%	1%	2%
	$\rho_{diff}^{B\ window}$	0.31	0.34	0.30	0.31
α^{*1F}	max Δ	0.10	0.11	0.04	0.04
	WMRE	6%	4%	1%	1%
	$\alpha_{diff}^{*1F\ window}$	0.28	0.31	0.50	0.60
α^{*2F}	max Δ	0.04	0.05	0.02	0.02
	WMRE	3%	3%	2%	1%
	$\alpha_{diff}^{*2F\ window}$	0.18	0.14	0.14	0.11
α^{*3F}	max Δ	0.005	0.004	0.002	0.002
	WMRE	3%	4%	2%	2%
	$\alpha_{diff}^{*3F\ window}$	0.029	0.023	0.024	0.017

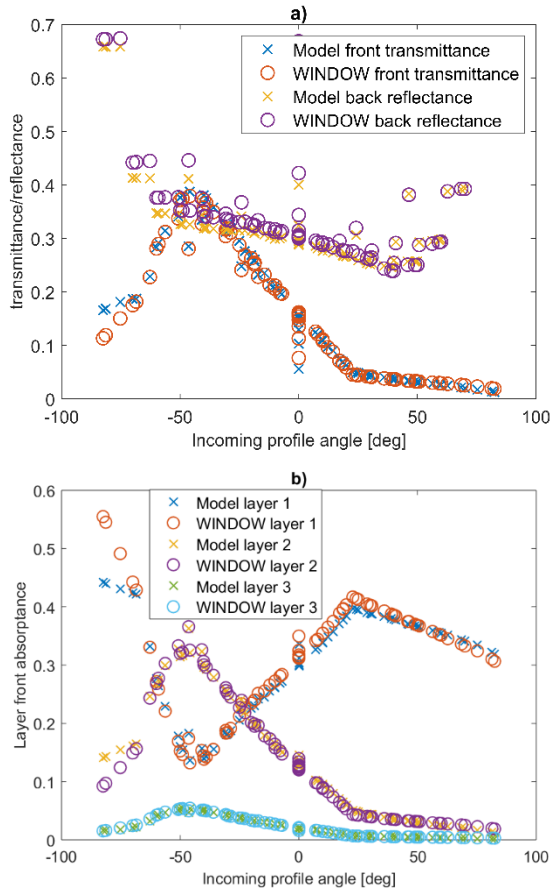

Figure 5 - Optical model validation, case B: a) window front transmittance and back reflectance b) layers absorbance (1 shading, 2 external glass, 3 internal glass)

Energy performances

In order to evaluate the multi-functionality and the overall energy performances of the new PV shading system the following indicators have been introduced and considered, comparing the results of the building simulation case study with the new and the reference window system defined in the previous section:

- Daylighting hours (DL)
- Net annual electrical (or equivalent) energy consumption for heating, cooling and lighting per floor unit area, including the exploitation of the PV generation:

$$E_{net} = \frac{1}{\eta_C}\mathrm{E}_C + \frac{1}{\eta_H}\mathrm{E}_H + \frac{1}{\eta_L}\mathrm{E}_L - \eta_E \mathrm{E}_{PV} \quad (9)$$

The E_{net} indicator is similar to the *energy balance index* introduced by [Oliviero at al. 2014]. Here E_C, E_H, E_L, E_{PV}, are respectively the specific annual energy need for cooling, heating, lighting and the PV generated, and $\eta_C, \eta_H, \eta_L, \eta_E$ are the corresponding system efficiency, assuming electrical supply/delivery. In this work, the energy needs and the PV generation have been dynamically simulated while the system efficiencies have been assumed as reported in Table 7. Considering such figures, the energy consumption related to the louvre mechanism movement is assumed to fall within the overall electrical system efficiency η_E.

Table 7 – Assumed cooling, heating, lighting and PV-exploitation efficiency

η_C	η_H	η_L	η_E
3	3.9	1	0.9

Parametric building simulations have been carried out to optimize the choice of the irradiance threshold G_{ST}, regarding the control strategy on the PV-louvres system. The overall results for seven threshold levels are reported in Table 8 and Figure 6, where the results for the reference building are reported for comparison as Case 8.

Table 8 – Building energy performances and daylight hours for system actuated with seven irradiance thresholds and for the benchmark

	G_{ST} W/m²	DL h	E_C/η_C kWh/(m²y)	E_H/η_H kWh/(m²y)	E_L/η_L kWh/(m²y)	$E_{PV}*\eta_E$ kWh/(m²y)	E_{net} kWh/(m²y)
1	100	1772	19.1	4.6	6.0	21.4	8.3
2	150	1886	19.2	4.6	5.2	21.4	7.5
3	200	1956	19.3	4.5	4.8	21.3	7.3
4	250	1998	19.6	4.5	4.5	21.1	7.4
5	300	2018	19.9	4.4	4.4	20.9	7.7
6	350	2034	20.1	4.4	4.3	20.7	8.1
7	400	2040	20.4	4.3	4.3	20.4	8.6
8		2093	22.1	3.7	3.9		29.7

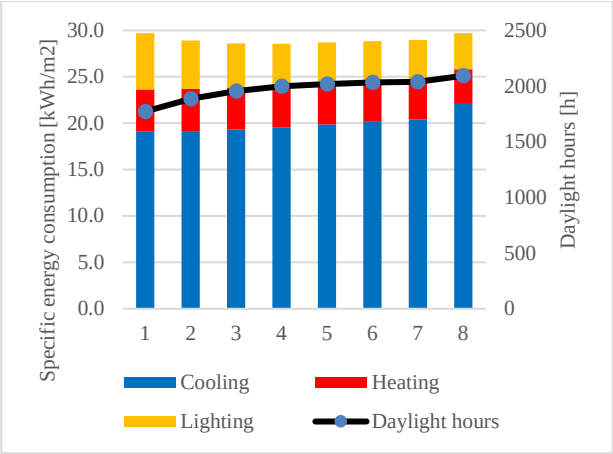

Figure 6 – Energy performance of the building and daylight hours for seven irradiance thresholds and the benchmark

The best option, based on the overall electrical energy index EP, is Case 3 with 75% of savings, which is due to a slight overall improvement in the energy efficiency and the significant contribution of the PV production. In Table 9 the daylight hours and the sensible heating and cooling demands are compared with the benchmark to highlight the contribution of the shading system to the energy balance. Furthermore, in the same table it is introduced the change in the energy use E_{use}, which is a balance of the total energy used for heating, cooling and lighting: as it does not include the PV, it gives a more precise idea of the performance of the proposed solution when regarded as traditional fenestration system.

Table 9 – Relative impact in daylight hours, sensible heating, sensible cooling, lighting, total use and net needs respect to the benchmark

	G_{ST} W/m²	DL	E_{SC}	E_{SH}	E_L	E_{use}	E_{net}
1	100	-15%	-35%	+63%	+56%	0%	-72%
2	150	-10%	-34%	+61%	+34%	-3%	-75%
3	200	-7%	-32%	+58%	+22%	-4%	-75%
4	250	-5%	-29%	+56%	+16%	-4%	-75%
5	300	-4%	-26%	+52%	+13%	-6%	-74%
6	350	-3%	-23%	+49%	+11%	-3%	-73%
7	400	-3%	-20%	+45%	+10%	-2%	-71%

The new extensible louvre system in Case 3, with GST equal to 200 W/m2, reduces the sensible cooling need of about one third, with a loss of daylighting availability of 7%. Even though the reduction in the transmitted solar energy affects both the heating and lighting demands, these are not dominant over the overall energy balance. Indeed, the energy performance of the reference building is characterized by very low heating demand, due to the high insulation and the internal gains typical of offices. It can be noted, that higher values of G_{ST} produce an even smaller reduction in daylight hours still providing a solar control somewhat improved respect to the benchmark.

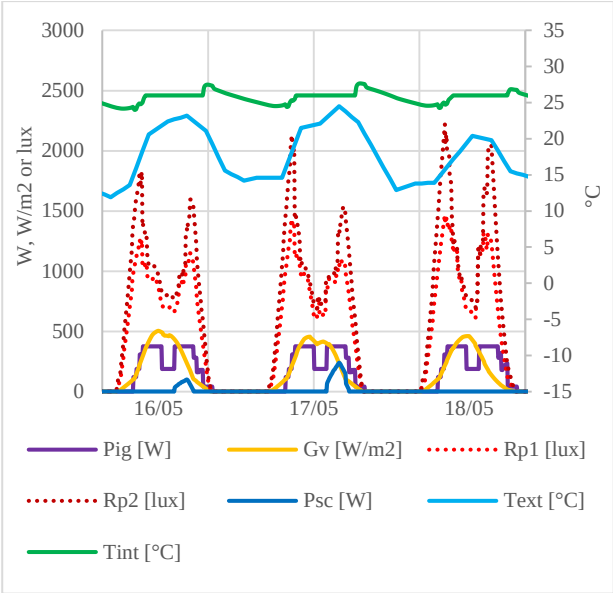

Figure 7 - Daily profiles of relevant parameters on May 16th,17th and 18th for Case 3, including internal gains power (Pig), irradiance on the façade (Gv), reference points illuminances (Rp1, Rp2), sensible cooling supply power (Psc), internal and external air temperatures (Tint, Text)

Figure 7, analysing the characteristic days in spring, shows how the activation of the control strategy reduce the solar loads and delays the need for cooling, while keeping the daylight level over the comfort level (600 lux threshold).

On top of this, decreasing the threshold irradiance in the control strategy means to give more Sun tracking freedom to the PV louvres: as shown in Table 10, this is reflected on a relative 4% increase of the PV performance ratio (PR_V), defined as

$$PR_V = \frac{E_{PV} * \eta_E}{H_V \eta_{PV}} \quad (10)$$

Where H_V is the yearly solar irradiation on the vertical surface and η_{PV} is the PV peak efficiency. In the same table, it is reported the PR_V for vertical modules: as in such configuration no partial shading appear, it can be used as a benchmark. The relatively high PR_V obtained with the extensible louvre is a combination of the exposure to the Sun (improved in summer and decreased in winter) and mismatch losses. Figure 8 shows three summer daily profiles of Case 3 power production in comparison with the vertical unshaded modules production and the reference maximum production of vertical module, which would happen at nominal efficiency. In such conditions, partial shading strongly decrease the energy production when Sun tracking is not active (i.e. morning and evening), while is nearly compensated by the better exposure the rest of the day. Furthermore, during the central hours no shadow affects the modules, thus improving the energy production respect to the vertical application thanks to Sun tracking.

Table 10 - PR_V of the PV system obtained for seven irradiance thresholds and for vertical modules

1	2	3	4	5	6	7	Vertical
0.72	0.72	0.72	0.71	0.71	0.70	0.69	0.85

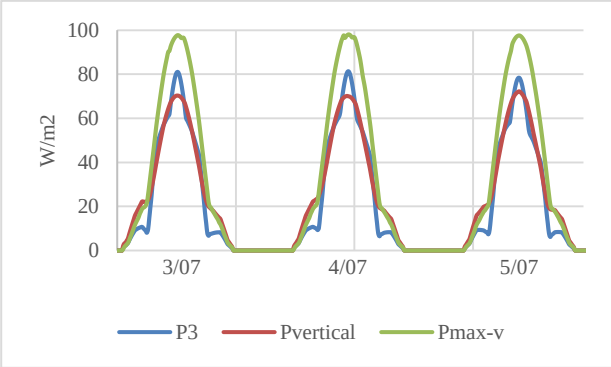

Figure 8 - PV power per unit module surface generated in Case 3 (P3) compared to generation of vertical modules (Pvertical) and to the reference power assuming vertical modules at nominal efficiency (Pmax-v) on July 3rd, 4th and 5th

Conclusions

This paper has provided a first assessment of the overall performances of dynamic complex fenestration systems integrating PV. In particular, the study is focused on an innovative BIPV louvre mechanism, whose shading surface regulation aims to adapt to the building daylighting and energy needs.

Firstly, it was validated an optical model for the bidirectional characterization of the complex fenestration system, based on the method employed in WINDOW software, suited to deal with the complex geometry of the innovative louvre and the combination of PV and blind materials.

Secondly, the use of an electrical-thermal PV model allowed to simulate the performances of the building integrated renewable energy system in a real environment. Simulations demonstrate how partial shading is affecting the yearly energy yield, thus highlighting the importance of the assumption regarding the PV system (i.e. technology, electrical connections and disposition over the louvre). In general, the PV performance is satisfactory for a semi-transparent application, thanks to the tracking possibility and the use of crystalline silicon technology.

Thirdly, the energy and daylighting performance of the system is simulated thanks to the integration of these two models into dynamic building simulations. The assessment of a proper control strategy allowed to reach a good compromise between daylighting and energy performances, leading to appreciable energy savings, in particular in sensible cooling. In fact, the louvers extension mechanisms allowed the system to provide effective solar control, with a very low impact on the daylight availability with respect to a benchmark based on standard in law.

Due to the relevance of this type of systems in reducing the energy consumption of some of the European building stock categories, it is important to continue the improvement in complex fenestration modelling and simulation. In particular, even though this paper demonstrates how complex and dynamic semi-transparent BIPV systems models can be integrated into whole building energy simulations, more effort should be done to improve the robustness of the tools and to extend the capability of simulating dynamical control of the building envelope elements.

Further developments include the implementation of a more sophisticated daylighting calculation method and of an improved control strategy as well as the integrated modelling of the building energy system (e.g. HVAC, PV electrical system, storage etc.). In this regard, timestep optimization of the control strategy (i.e. based on actual internal daylighting and temperature levels) and model predictive controls would offer ample room for improvement.

Furthermore, in order to estimate the potential application of the proposed shading system and modelling methodology, different building typologies and climatic conditions should be considered as well.

Nomenclature

α_i^{1F}	front absorptance of layer 1 for entering direction *i*, when characterized alone
$\alpha^*_i{}^{1F}$	front absorptance of layer 1 for entering direction *i*, when included in a fenestration system
$\alpha^*_{diff}{}^{1F}$	front absorptance of layer 1 for diffuse irradiance, when included in a fenestration system
ψ_i	angular weight in the hemisphere for direction *i*
ρ_{ij}^{1B}	back reflectance of layer 1 for entering direction *i* and outgoing direction *j*
ρ_i^{1B}	back hemispheric reflectance of layer 1 for entering direction *i*
ρ_{diff}^{1B}	back hemispheric reflectance of layer 1 for diffuse irradiance
τ_{ij}^{1F}	front transmittance of layer 1 for entering direction *i* and outgoing direction *j*
τ_i^{1F}	front hemispheric transmittance of layer 1 for entering direction *i*
τ_i^{1F}	front hemispheric transmittance of layer 1 for diffuse irradiance
A^{1F}	vector of $\{a_i^{1F}\}$
R^{1B}	matrix of $\{\rho_{ij}^{1B}\}$
T^{1F}	matrix of $\{\tau_{ij}^{1F}\}$
max Δ	maximum absolute error
WMRE	Weighted Mean Relative Error
$E_{C/H}$	Cooling/Heating Energy needs
E_L	Electtric lighting need
E_{PV}	PV generation

G_V vertical irradiance on the facade

G_{ST} solar tracking irradiance threshold

References

Alonso-Garcia, M.C., Ruiz, J.M., Herrmann, W., Computer simulation of shading effects in photovoltaic arrays, 2006, Renewable Energy 31, 1986-1993

Curcija, C., Vidanovic, S, Hart, R., Jonsson, J., Mitchell, R., WINDOW technical documentation, 2018, LBNL, Berkley, CA, USA

Dama A. and Lastaria F., 'Explicit versus implicit method for radiative heat transfer in gray and diffuse enclosures', Int. J. Heat Mass Transf., vol. 55, no. 13–14, pp. 3829–3833, Jun. 2012.

Liu, G., Nguang, S. K., Partridge, A., A general modelling method for I-V characteristics of geometrically and electrically configured photovoltaic arrays, 2011, Energy Conversion and Management 52, 3439-3445

Olivieri, L., Caamaño-Martín, E., Moralejo-Vázquez, F. J., Martín-Chivelet, N., Olivieri, F., & Neila-Gonzalez, F. J. (2014). Energy saving potential of semi-transparent photovoltaic elements for building integration. *Energy*, *76*, 572–583.

Peng, J., Jonsson, J., Hart, R., Curcija, D.C., Selkowitz, S. E., Parametric study of window attachment impacts on building heating/cooling energy consumption, 2017, Proceedings of the 15th IBPSA Conference, San Francisco, CA, USA

Piccoli, E., Dama, A., Shading device with extensible louvres for daylighting and solar control, 2018, Proceedings of the 13th Conference on Advanced Building Skins, 1-2 October 2018, Bern, Switzerland, pp. 770-779

Piccoli, E., Dama, A., Dolara, A., Leva, S., 2019, Experimental validation of a model for PV systems under partial shading for building integrated applications, Solar Energy, Vol. 183, pp. 356-370